Investigation of transient electric and magnetic fields associated to the propagation of relativistic electron currents

M. Borghesi, P. A. Wilson, C. A. Cecchetti and S. Kar
School of Mathematics and Physics, The Queen's University, Belfast, BT7 1NN, UK

J. Fuchs, P. Antici and L. Romagnani
Laboratoire pour l'Utilisation des Laser Intenses (LULI) CNRS-Ecole Polytechnique-Univ, Paris, France

O. Willi, R. Jung, J. Osterholtz and C. A. Pipahl
Insitut für Laser-und Plasmaphysik, Heinrich-Heine-Universität, Düsseldorf, Germany

M. Tampo, H. Nakamura and R. Kodama
Institute of Laser Engineering, Osaka University, Osaka, Japan

W. Nazarov
School of Chemistry, University of St Andrews, St Andrews, UK

S. Bandyopadhyay, M. Notley and M. Tolley
Central Laser Facility, CCLRC Rutherford Appleton Laboratory, Chilton, Didcot, Oxon., 0X11 0QX, UK

Main contact email address m.borghesi@qub.ac.uk

Introduction

Ultra short bursts of high-energy charged particles are produced from high-intensity laser matter interactions, and have many potential applications in advanced science and technology areas[1]. A crucial application of laser-produced MeV electrons is in Inertial Confinement Fusion via Fast Ignition of a pre-compressed fuel[2,3]. Recently, the Fast Ignitor community has focused its attention on a scheme employing a re-entrant cone, which has led to significant increase in neutron yields in experiments performed at ILE, Osaka[4]. By concentrating all the laser energy at the tip of the cone, this scheme was initially envisioned as a way to circumvent the effect of inhomogeneities in the laser focal spot and non-perfect illumination of the imploded target, detrimental to the laser-coupling efficiency. An additional benefit of the cone geometry seems to be the capability of enhancing conversion efficiency into fast electrons and ions[5]. Also, the re-entrant cone geometry could allow fast electron production close to the dense core, reducing electron propagation issues through the dense plasma surrounding it. The propagation of relativistic electrons through dense matter is however a subject still attracting a great deal of experimental and theoretical attention. Scaling laws for the hot electrons produced during ultrahigh intensity interactions give $K_B T_{hot} \sim U_{pond} \sim 1$ MeV • $(I\lambda^2/10^{19} \mathrm{Wcm^{-2}}\ \mu m^2)^{0.5}$, with up to 30% of the laser energy converted in these relativistic electrons. There is debate on the behaviour of such large currents inside matter, and on the extent to which electromagnetic instabilities will be detrimental to their propagation.

A recent experiment has shown that, by adding a thin wire at the tip of a cone one can actually guide a relativistic electron current from the tip of the cone along the wire, effectively creating a guiding device for relativistic electrons with enormous potential for applications[6]. According to simulations interpreting the experimental results, the interplay of electric and magnetic fields near the surface of the wire provides the crucial conditions for collimating and confining the electron flow. Recent work has also highlighted several interesting features of proton acceleration from cone-wire assemblies[7].

Here we report the first results of a campaign investigating the transient fields associated to relativistic electron current flow in cone-wire assemblies and solid/foam targets. These studies were carried out employing the now well-established technique of proton imaging[8], able to provide high-resolution snapshots of the electric and magnetic field distribution present in and around a laser-irradiated target.

Experimental arrangement

The experiment was carried out at the Vulcan Laser, Rutherford Appleton Laboratory. The dual CPA configuration was employed, providing two CPA pulses with adjustable relative delay. By using f/6 off axis parabolas, the beams were focussed down, on two separate targets (*interaction target* and *proton target*), within a focal spot of radius 10 μm. The peak intensity delivered on target was up to 2×10^{19} W/cm^2.

Throughout the experiment we employed a variety of interaction targets. Re-entrant cones with a solid CD fibre assembled to the disc at the tip of the cone were used, with the aim of detecting electric and magnetic fields arising near the wire and cone surface (Fig 1). The cone target was made by assembling a gold disc 10 μm thick and 30 μm in diameter at the tip of a 1mm long and 10 μm thick gold re-entrant cone with an opening angle of 30°. The CD fibres were 20 μm in diameter, with length either 0.3 mm or 1 mm. One end of the fibre was glued to the centre of the disk at the tip of the cone.

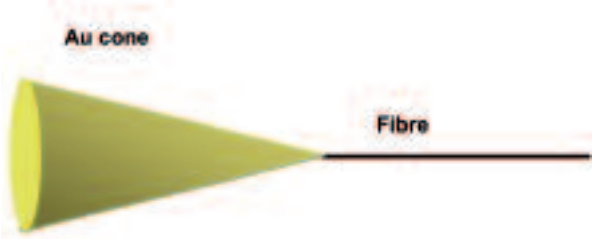

Figure 1. Typical cone –fibre target: The target consists of a Au re-entrant cone with 30° open angle terminating in a flat 30 μm diameter disk, to which a CD fibre is attached.

In order to detect fields associated to the flow of electrons in the bulk of dense matter we used solid and foam targets. Proton probing of dense matter is affected by scattering, which can significantly reduce the spatial resolution of the diagnostic[9] and inhibit the detection of small-scale field structures. In order to obtain meaningful data, it is therefore crucial to minimize the amount of matter the protons have to cross. To this purpose we employed *laminar* targets, i.e. targets extending much more in the longitudinal direction (the laser propagation axis) than in the transverse direction (the proton probe axis). We used a variety of foam targets: triacrylate ($C_{15}H_{20}O_6$) foams of various densities (20 to 200 mg/cc) were deposited in an Aluminium half-washer of internal diameter 1.5 mm and thickness 300 µm (see fig.2), with its sides closed by a 8 µm plastic foil. In a very limited number of shots we employed 60 µm thick, mm-long plastic foils, suitably shielded (data not discussed here).

The schematic diagram of the experimental arrangement is shown in Fig 3. Fig.3 shows the arrangement used for probing cone-fibre targets, but the set-up for laminar target probing was analogous. One of the two CPA beams is employed to generate the probe proton beam by irradiating a flat foil of 25 µm Au.

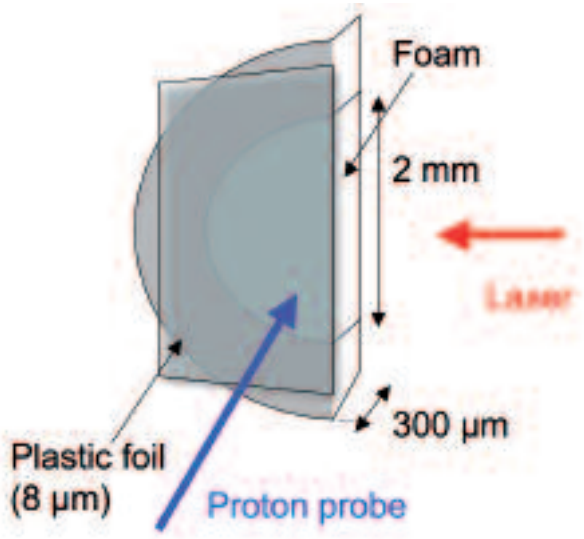

Figure 2. Schematic diagram of foam target. Tryacrylate ($C_{15}H_{20}O_6$) foam is enclosed in an Al washer of internal diameter 2 mm and thickness 0.3 mm. A plastic foil of thickness 8 µm is used to close the side of the washer.

The other CPA beam was used as the interaction beam. Each beam could deliver energies up to 50 J, but the energy delivered in the cone targets was limited to 5-10 J in order to reduce target charge-up[10].

The interaction target was probed transversely by the proton probe beam. In some shots, a Cu mesh was inserted between the proton source and the interaction target in a proton deflectometry arrangement[11].

The detector used was a stack of Radiochromic film (RCF), placed at a distance of 31mm from the interaction target, giving a magnification of about 9 for a separation of 4 mm between the two targets. The RCF films provided a multi-frame record of the temporal evolution of the fields around the target as each film is at a different depth in the film stack, detects protons of different energy and

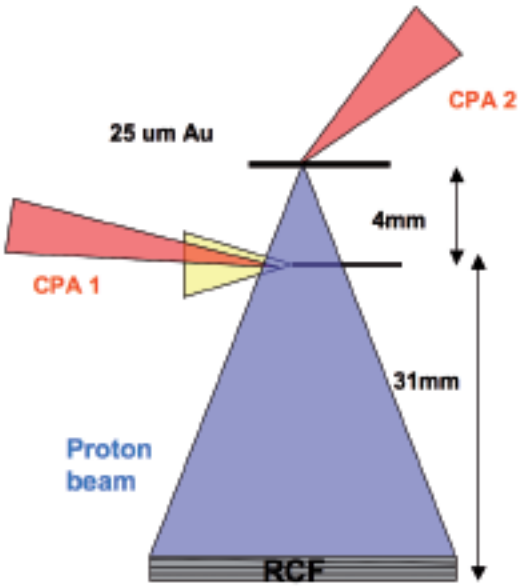

Figure 3. Schematic diagram of experimental arrangement. A dual CPA configuration is used, where one of the CPA beam is used to generate the proton probe whilst the other CPA beam is used as interaction beam.

therefore carries information relating to a different stage of the interaction target evolution[8]. The time of arrival of protons at the interaction plane was controlled by a double pass timing slide, inserted in the path of CPA_1, before final amplification.

The interaction target was also diagnosed by Nomarsky interferometry and shadowgraphy diagnostics, employing a frequency doubled CPA probe pulse. A pinhole camera observed the interaction point, and other diagnostics, not discussed here, detected the neutrons emitted from the CD wire, and the spectrum and angular emission of the electrons from cone-wire assemblies.

Experimental results

In this section some examples of results obtained during this experiment are shown. The analysis of this data is ongoing, therefore we will limit ourselves to highlighting some of the features observed.

Fig 4 shows the proton images obtained on consecutive RCF layers of a multilayer pack, corresponding to different times relative to the interaction with a cone-wire target.

While in the first layer (snapshot taken ~ 11 ps before the interaction) one observes the shadow of the unperturbed target, closer to the interaction several evolving deflection patterns can be seen. The interpretation of the complex deflection pattern will require extensive particle tracing simulations, possibly coupled to Particle in Cell modeling, however we can tentatively describe some of the features observed.

An almost stationary halo surrounds the cone and fibre (clearly visible in frames c) and d) and already developing several ps before the interaction pulse peak (frame b)), likely to be due to proton deflection associated to whole charge-up of the target, following ejection of electrons[10]. Large magnetic fields surrounding the wire[4] may also contribute to the depletion region around the wire surface observed in the proton images taken after the interaction pulse peak. We

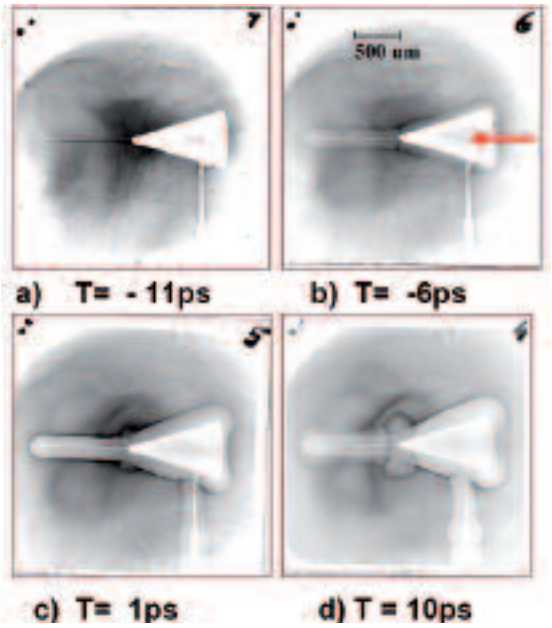

Figure 4. RCF data providing information on the field distribution following the interaction with a cone-fibre target assembly. The times shown underneath each layer are the nominal probing time for protons reaching the Bragg peak in the layer, relative to the arrival of the interaction pulse on target (with timing precision of a few ps). The red arrow indicates the CPA irradiation direction.

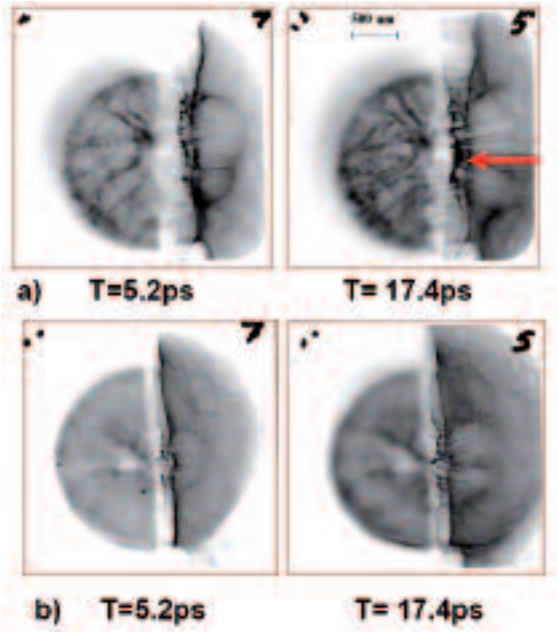

Figure 5. RCF images of foam targets following CPA interaction. The density of the foam was 50mg/cc for images in the top row, 200mg/cc in the bottom row. The hemi-circular shadow on the left side of the images is due to the half-washer enclosing the foam (see fig.2), while the vertical white line at the centre of the images corresponds to the foam-vacuum interface. Beside plasma expansion from the interface into the vacuum, the images clearly show features appearing inside the bulk of the target.

expect that a detailed analysis of this and similar data, and in particular of proton deflectograms, will enable discriminating between the contribution of radial electric fields and azimuthal magnetic fields to the observed patterns.

Two lobes expanding above and below the tip of the cone are observed in frames c) and d) and are likely to be related to an expanding disk-like ion front, moving with velocity of the order of 10^7 m/s (e.g. corresponding to a ~MeV proton front). The effect of this front on the proton probe is via the associated electric field structure, as discussed for example in[11]. An expanding front surrounding the fibre, is also seen (clearly visible in frame 4 where it extends around the halo mentioned previously).

Shots employing laminar solid and foam targets can provide novel information on the propagation characteristics of relativistic electrons inside matter. Previous studies of laser-driven electron propagation through transparent solids[12,13] were carried out by observing the induced target ionization effects via optical shadowgraphy. These experiments showed filamentary ionization and the propagation of a diffusive ionization wave, with the target becoming opaque very soon after the interaction. Proton probing can provide direct information on the fields set-up by the relativistic electron current and the cold, neutralizing return current driven from the bulk of the target.

Data from foam target shots are shown in fig. 5 (top row and bottom row show data from interaction with foams of density 50mg/cc and 200mg/cc respectively). The laser pulse is incident from the right, and fields associated to fast plasma expansion in vacuum[11] can be observed on the right side of the images. The data also shows structures appearing inside the target after the interaction, most likely associated to the propagation of relativistic electron created by the laser pulse interaction with the target surface, which will penetrate into the target bulk and ionize it. The structures extend for several hundreds of microns and are contained within a ~45° opening half-angle for the 50 mg/cc data, and a 30° half-angle for the 200 mg/cc data. Although the observed features appear suddenly around the interaction peak, some evolution is also observed after the interaction. Modelling of the interaction and electron propagation inside the target, and of its effect on driving returns currents the target bulk (e.g. using the approach suggested in[14]), will help clarifying the dynamics observed and the nature of the fields (electric or magnetic) causing the proton deflections.

References

1. G. A. Mourou, T. Tajima, S. V. Bulanov, *Rev Mod. Phys*, **78**, 309 (2006)
2. M. Tabak *et al*, *Phys. Plasmas*, **1**, 1626 (1994)
3. S. Atzeni, *Phys. Plasmas*, **6**, 3316 (1999)
4. R. Kodama *et al*., *Nature* **432**, 1005 (2004)
5. Z. L. Chen *et al*, *Phys. Rev. E* **71**, 036403 (2005)
6. R. Kodama *et al*, *Nature* **432**, 1005 (2004).
7. Z. L. Chen *et al*, *Phys. Rev. Lett*., **96**, 084802 (2006)
8. M. Borghesi *et al*, *Phys. Plasmas*, **9**, 2214 (2002)
9. A. J. Mackinnon *et al*, *Phys. Rev. Lett*., **97**, 045001 (2006)
10. M. Borghesi *et al*, *App. Phys. Lett*., **82**, 1529 (2003)
11. L. Romagnani *et al*., *Phys. Rev. Lett*., **95**, 195001 (2005)
12. M. Borghesi *et al*., *Phys. Rev. Lett*., **83**, 4309 (1999)
13. L. Gremillet *et al*, *Phys. Rev. Lett*., **83**, 5015 (1999)
14. R. G. Evans, *CLF Annual Report 2004-2005*, p.94